STABLE EOCENE MAGNETIZATION CARRIED BY MAGNETITE AND IRON SULPHIDES IN MARINE MARLS (PAMPLONA-ARGUIS FORMATION, SOUTHERN PYRENEES, NORTHERN SPAIN)

J.C. LARRASOAÑA[1,2,*], J.M. PARÉS[3], E.L. PUEYO[1,2,**]

1 Paleomagnetic Laboratory, Institute of Earth Sciences "Jaume Almera", CSIC, Solé i Sabarís s/n, Barcelona 28080, Spain
2 Department of Earth Sciences, University of Zaragoza, c/ Pedro Cerbuna 12, Zaragoza 50009, Spain
3 Department of Geological Sciences, University of Michigan, 1006 C. C. Little Building, Ann Arbor, MI 48109, USA, jmpares@j.imap.itd.umich.edu
* Corresponding author. Now at: Southampton Oceanography Centre, European Way, Southampton SO14 3ZH, UK, jcl1@soc.soton.ac.uk
** Now at: Paleomagnetic Laboratory, Institut of Geophysics, Montanuniversität Leoben, Gams 45, A-8130, Austria, pueyo@unileoben.ac.at

Received: June 8, 2002; Accepted: February 7, 2003

ABSTRACT

In order to establish the magnetic carriers and assess the reliability of previous paleomagnetic results obtained for Eocene marine marls from the south Pyrenean basin, we carried out a combined paleo- and rock-magnetic study of the Pamplona-Arguis Formation, which crops out in the western sector of the southern Pyrenees (N Spain). The unblocking temperatures suggest that the characteristic remanent magnetization (ChRM) is carried by magnetite and iron sulphides. The ChRM has both normal and reversed polarities regardless of whether it resides in magnetite or iron sulphides, and represents a primary Eocene magnetization acquired before folding. Rock magnetic results confirm the presence of magnetite and smaller amounts of magnetic iron sulphides, most likely pyrrhotite, in all the studied samples. Framboidal pyrite is ubiquitous in the marls and suggests that iron sulphides formed during early diagenesis under sulphate-reducing conditions. ChRM directions carried by magnetic iron sulphides are consistent with those recorded by magnetite. These observations suggest that magnetic iron sulphides carry a chemical remanent magnetization that coexists with a remanence residing in detrital magnetite. We suggest that the south Pyrenean Eocene marls are suitable for magnetostratigraphic and tectonic purposes but not for studies of polarity transitions, secular variations and geomagnetic excursions, because it is difficult to test for short time differences in remanence lock-in time for the two minerals. The presence of iron sulphide minerals contributing to the primary magnetization in Eocene marine marls reinforces the idea that these minerals can persist over long periods of time in the geological record.

Keywords: paleomagnetism, rock magnetism, marine sediments, early diagenesis, magnetic iron sulphides, Pyrenees

1. INTRODUCTION

The co-occurrence of magnetite with the ferrimagnetic iron sulphides greigite (Fe_3S_4) or pyrrhotite (Fe_7S_8) has important implications for the reliability of paleomagnetic data as carriers of primary magnetizations in marine sedimentary environments (e.g., *Roberts and Turne,r 1993*; *Verosub and Roberts, 1995*; *Horng et al., 1998*). Under reducing conditions during deposition and earliest diagenesis, greigite and pyrrhotite can grow authigenically as a precursor in the formation of pyrite (*Sweeney and Kaplan, 1973*; *Berner, 1984*). Dissolution of detrital magnetite grains usually occurs during this process (*Canfield and Berner, 1987*; *Karlin, 1990*; *Leslie et al., 1990*). As a result, a chemical remanent magnetization (*ChRM*) carried by magnetic iron sulphides might coexist with a detrital magnetization carried by magnetite that survived dissolution (*Roberts and Turner, 1993*; *Horng et al., 1998*). However, greigite and pyrrhotite can also form at later diagenetic stages (*Reynolds et al., 1991*; *Florindo and Sagnotti, 1995; Housen and Musgrave, 1996*; *Dinarès-Turell and Dekkers, 1999*; *Jiang et al., 2001*; *Weaver et al., 2002*), which results in either delayed primary remanences (*van Hoof and Langereis, 1991*) or in secondary magnetizations (e.g., *Horng et al., 1998*). Detrital magnetite might undergo complete dissolution during this process, in which case the natural remanent magnetization (*NRM*) recorded by a sediment might lack any reliable information about the behaviour of the Earth's magnetic field at the time of deposition. Knowledge about the occurrence and origin of magnetic iron sulphides, made possible after development in the last few years of new techniques and approaches (e.g., *Krs et al., 1990,1992*; *Roberts and Turner, 1993*; *Verosub and Roberts, 1995*; *Torii et al., 1996*; *Horng et al., 1998*; *Jiang et al., 2001*), is therefore important for checking the reliability of paleomagnetic data from marine sediments that contain these minerals.

The external units of the southern Pyrenees (northern Spain) are characterized by thick (up to 2000 m) Eocene marine sequences mainly composed of bluish marls. Several magnetostratigraphic (*Burbank et al., 1992a,b*; *Bentham, 1992*; *Hogan, 1993*; *Hogan and Burbank, 1996*; *Taberner et al., 1999*) and magnetotectonic (*Dinarès-Turell et al., 1992; Holl and Anastasio, 1993; Pueyo et al., 1997,2002,2003*; *Larrasoaña et al., 2003*) studies carried out on these marls have shown that magnetite is the main remanence carrier, although the unblocking temperatures indicate that magnetic iron sulphides might also contribute to the characteristic remanent magnetization (*ChRM*). The lack of detailed rock-magnetic analysis has prevented, however, an accurate determination of the type and origin of the iron sulphides in these marls, and therefore their reliability as paleomagnetic carriers is still to be fully tested. To cover this gap, we present the first combined paleo- and rock-magnetic study of the marine Eocene marls, carried out at the western sector of the southern Pyrenean basin, in the so-called Pamplona-Arguis Formation.

2. GEOLOGICAL SETTING

The Pamplona-Arguis Formation (PAF) crops out along the western sector of the south Pyrenees, in the so-called Jaca-Pamplona basin (Fig. 1). This basin constitutes a south-vergent synclinorium that overrides the Ebro Foreland Basin along the South Pyrenean Frontal Thrust (SPFT), and is affected by a set of minor folds and thrusts developed from Middle Eocene to Miocene times. From the Late Cretaceous to the

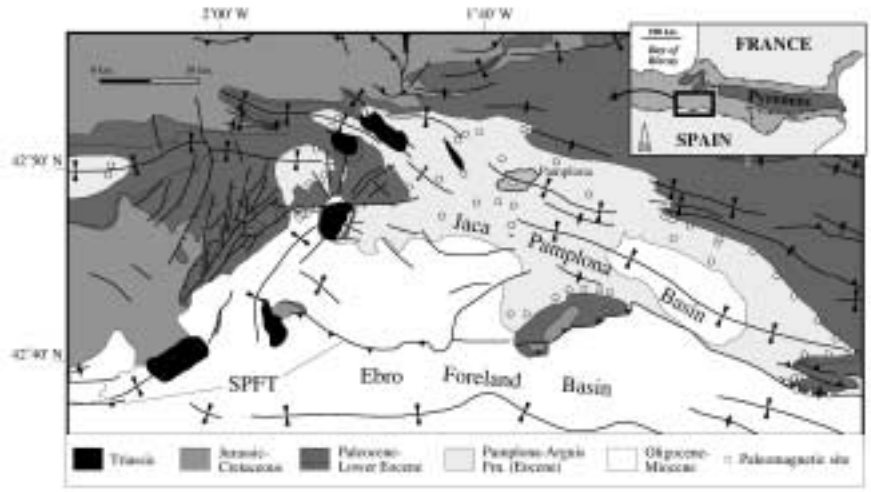

Fig. 1. Geological sketch map of the western sector of the Jaca-Pamplona basin, with location of the studied sites (open circles). SPFT: South Pyrenean Frontal Thrust.

Eocene, the Jaca-Pamplona basin formed as a subsiding foreland basin in response to tectonic loading of the internal units of the Pyrenees to the north (*Teixell, 1996*). The PAF comprises a monotonous sequence of bluish marine marls, which were deposited during the Middle-Late Eocene in the distal part of a deltaic system that opened toward the west-northwest (*Puigdefàbregas, 1975*). Prodeltaic, relatively deep marly facies are typical throughout the stratigraphic pile, although some reefal and turbiditic levels are also present in the south-eastern and westernmost sectors of the basin (*Puigdefàbregas, 1975*; *Millán et al., 1994*). The thickness of the formation decreases toward the south, ranging between 1000–2000 m in the northern margin of the basin and 200–1000 m towards the south. Biostratigraphic (*Canudo et al., 1988*) and magnetostratigraphic data (*Hogan and Burbank, 1996*) indicate an age of Bartonian-lower Priabonian for this formation. This gives a mean sediment accumulation rate of about 30 cm/kyr, which progressively increases throughout the stratigraphic pile (from 5 cm/kyr at the base to 50 cm/kyr at the top) due to increasing tectonic subsidence of the basin (*Millán et al., 1994*). In the studied area, the PAF is overlain by a sequence of up to 3000 m of Oligocene-Miocene continental deposits (*Puigdefàbregas, 1975*).

3. SAMPLING AND LABORATORY PROCEDURES

Standard oriented cores (25.4 mm diameter) of Eocene marls were collected with a portable gas drill in the western sector of the Jaca-Pamplona basin (Fig. 1). Eight to 15 cores were collected at 55 sites. At every site, a stratigraphic thickness of several (up to 15) meters was sampled. Cores were cut in the laboratory to obtain standard paleomagnetic specimens (22 mm length).

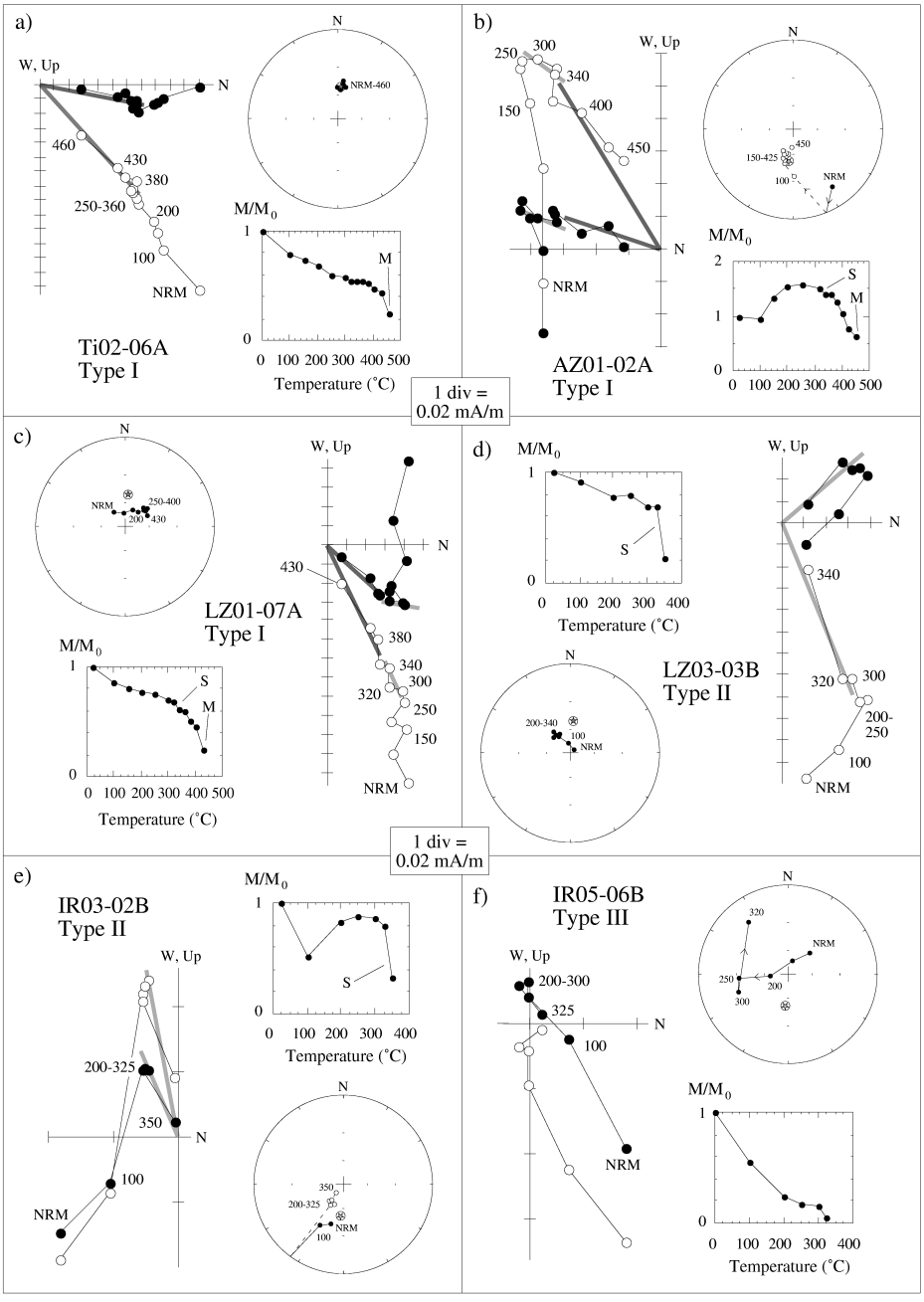
a)
W, Up
N
460
430
380
250-360
200
100
NRM
NRM-460
M/M0
1
0
M
0 100 200 300 400 500
Temperature (˚C)
Ti02-06A
Type I
b)
W, Up
250
300
340
400
150
450
N
NRM
150-425
100
NRM
M/M0
2
1
0
S
M
0 100 200 300 400 500
AZ01-02A
Type I
1 div =
0.02 mA/m
c)
NRM
250-400
200
430
LZ01-07A
Type I
M/M0
1
0
S
M
0 100 200 300 400 500
Temperature (˚C)
W, Up
N
430
380
340
300
320
250
150
NRM
d)
M/M0
1
0
S
0 100 200 300 400
Temperature (˚C)
200-340
100
NRM
LZ03-03B
Type II
W, Up
N
340
320
300
200-
250
100
NRM
1 div =
0.02 mA/m
e)
IR03-02B
Type II
W, Up
200-325
350
N
100
NRM
M/M0
1
0
S
0 100 200 300 400
Temperature (˚C)
350
200-325
NRM
100
f)
IR05-06B
Type III
W, Up
200-300
325
N
100
NRM
320
NRM
250
200
300
M/M0
1
0
0 100 200 300 400
Temperature (˚C)

Measurements of magnetic remanence were made using three-axis cryogenic magnetometers at the CSIC in Barcelona (GM400), the Ludwig-Maximilians University in Munich (2G) and the University of Michigan in Ann Arbor (2G). The noise level of these magnetometers is less than 7×10^{-6} A/m, which is well below the magnetization of most of the measured samples. Stepwise thermal demagnetization of the *NRM* was carried out with Schonstedt and ASC furnaces at 50º, 30º and 20º intervals up to 500ºC. Low-field magnetic susceptibility was measured after each heating step using KLY-2 (AGICO Ltd.) susceptibility meters in order to detect formation of new magnetic phases during thermal treatment.

Rock magnetic analyses were performed on selected whole-rock samples at the paleomagnetic laboratory at the Ludwig Maximilians University and at the Institute for Rock Magnetism at the University of Minnesota (USA). At the Ludwig Maximilians University, thermomagnetic runs between 30º and 700ºC (heating rate of ~ 40º/min; 0.3 T) were performed on rock-powder samples using a variable field translation balance VFTB. An isothermal remanent magnetization (*IRM*) was imparted at progressively increasing fields up to 1.5 T with a pulse magnet. An anhysteretic remanent magnetization (*ARM*) was acquired (using a 2G in-line system) in a bias field of 0.05 mT and a peak alternating field (AF) of 250 mT applied in the same direction. The decay of *ARM* and *IRM* intensities during incremental AF demagnetization was measured using cryogenic and Molspin magnetometers, respectively. Thermal demagnetization of a three-component *IRM* (*Lowrie, 1990*) was also measured with a cryogenic magnetometer.

At the Institute for Rock Magnetism (Minneapolis, USA), thermomagnetic runs between 30° and 700°C (heating rate of 20–30°/min; 0.3 T) were carried out in air and in He atmosphere using a Princeton Measurements Corporation Micro-Vibrating Sample Magnetometer (μVSM). B_c, M_s and M_{rs} were calculated from room temperature hysteresis loops, which were also performed on chip-rock samples with the same μVSM. B_{cr} was determined from back-field measurements. Low temperature (10–300 K) measurements of saturation remanent magnetization (M_{rs}) were performed using a Quantum Designs Magnetic Properties Measuring System (MPMS). Low-temperature measurements of M_{rs} induced at 2.5 T and 10 K were conducted upon heating the sample back to room temperature after the removal of the applied field. Two heating runs were conducted, the first one involving previous cooling of the samples down to 10 K in the absence of any magnetic field (ZFC) and the second one involving the application of a 2.5 T field during initial cooling (FC) (Fig. 5).

Fig. 2. (facing page) Representative demagnetization plots of Eocene marls: type I samples with (a, c) normal and (b) reversed polarities; type II samples with (d) normal and (e) reversed polarities; type III sample (f) where no reliable *ChRM* direction could be determined. Solid (open) symbols represent horizontal (vertical) projections. Dark (light) grey lines indicate the line fit of the *ChRM* unblocked above (below) 350˚C. The decay of *NRM* as a function of temperature and the stereographic projection of the demagnetization results are also shown. Solid (open) symbols and solid (dashed) lines indicate points and paths in the lower (upper) hemisphere. The star indicates the Eocene reference direction. S and M indicate the decay probably associated to magnetic iron sulphides and magnetite, respectively. All plots are shown after tilt correction. Above 400˚–450˚C, new magnetic minerals are formed, which leads to strong spurious magnetizations with inconsistent directions. These data are not shown.

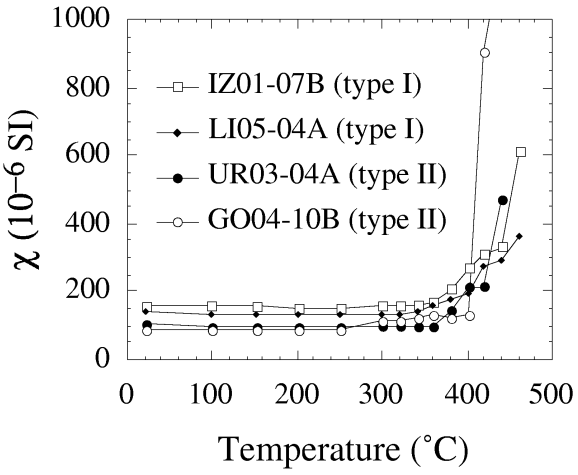

Fig. 3. Variations of low-field magnetic susceptibility from representative samples upon thermal demagnetization.

Representative thin sections were prepared for scanning electron microscope (Stereoscan 120, Cambridge Instruments) observations at the University of Barcelona. Iron-bearing minerals were first located with a backscattered electron (BSE) detector, and were later analyzed with an energy dispersive analysis system (EDS). Some selected samples were prepared for transmission electron microscopy (TEM) observations using an ion mill to produce thin edges (Hitachi 800MT). This TEM provides selected area electron diffraction (SAED) patterns for definition of crystal structure. X-ray diffraction (XRD) analysis performed at the CSIC in Barcelona were carried out on some rock-powder samples.

4. RESULTS

4.1. Paleomagnetism

The initial *NRM* intensity of the PAF marls usually ranges between 0.1 and 0.6 mA/m, although some samples show extreme values of about 0.03 mA/m and 1.8 mA/m. Stepwise thermal demagnetization of over 500 specimens indicates that two stable components can be identified in the majority of the samples (Fig. 2). Formation of new magnetic phases above 350–400°C is revealed by an increase in the low-field magnetic susceptibility (Fig. 3), and often prevented the complete demagnetization of the samples. However, linear paths directed toward the origin of the orthogonal plots could be identified with confidence in about 75% of the measured specimens (Fig. 2a-d). Three main groups of samples have been distinguished on the basis of their paleomagnetic behaviour. The three groups are characterized by a low temperature component that typically unblocks below 300°C. Before tilt correction, this component is parallel to the

present-day field direction in the area (D = 000°, I = 60°) and is therefore interpreted as a recent overprint. The first group, referred to as type I, has a *ChRM* that unblocks from above 250–300°C (Fig. 2a). In several cases, a subtle drop in the *NRM* can be observed below 350°C (Fig. 2b-c). In the second group of samples (type II), the *ChRM* distinctively unblocks below 350°C (Fig. 2d-e). *ChRM* intensities of type I samples are higher, although they are still comparable, to those of type II samples. The third group of samples (type III) is characterized by unstable behaviour above 300°C, which prevented calculation of reliable *ChRM* directions (Fig. 2f). The intensity of the *NRM* remaining after 300°C in type III samples is much lower than at the same demagnetization level in type I and II samples. Type I samples represent about 65% of the analyzed samples, whereas types II and III account for the remaining 10% and 25% of the samples, respectively. Samples with different behaviour appear mixed at the outcrop (and even at the paleomagnetic sample) scale, although type II and III samples are more common in the middle and upper parts of the stratigraphic pile and type I samples are predominant in the lowermost levels.

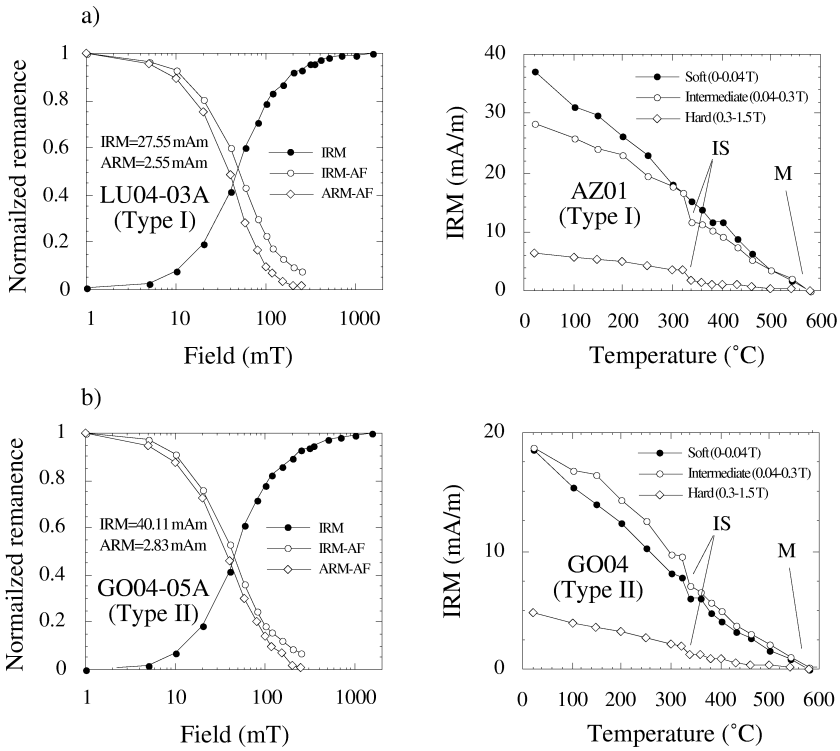

Fig. 4. a) *IRM* acquisition curves and AF demagnetization curves for the *ARM* and *IRM*, b) Thermal demagnetization of a three-component *IRM* for representative samples showing type I and II behaviour. S and M indicate magnetic iron sulphides and magnetite, respectively.

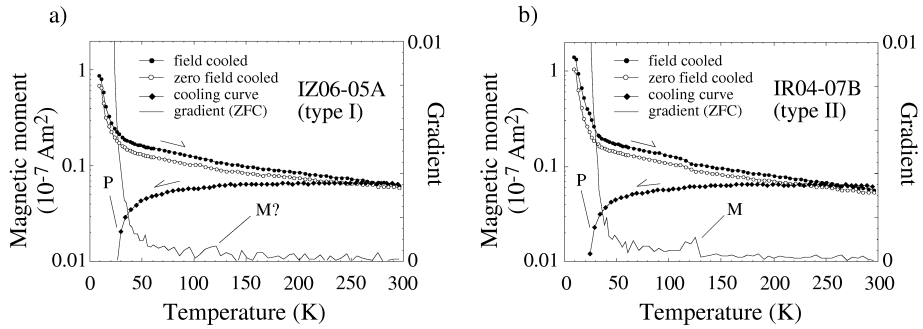

Fig. 5. Low-temperature *IRM* curves from two representative samples with type I and II behaviour. P and M indicate the low-T transitions of pyrrhotite and magnetite, respectively.

4.2. Rock magnetism

Rock magnetic experiments were aimed at determining the magnetic mineralogy of samples from sites with stable remanences (types I and II). All studied samples of both types have very similar rock magnetic properties (Figs. 4–7). About 80% of the *IRM* is acquired at fields of 100 mT, with only minor acquisition of remanence above 300 mT (Fig. 4). In all samples, the *IRM* is slightly more resistant to AF demagnetization than the *ARM*. Representative plots of the thermal demagnetization of a three-component *IRM* are shown in Fig. 4b. The soft (up to 40 mT) and the intermediate (40–300 mT) components have similar intensities and show a complete decay of remanence at 580°C. An additional weak, but distinctive decay of *IRM* at 340°C is usually observed in both components, although it is clearer in the intermediate component. The hard component (0.3–1.5 T) has

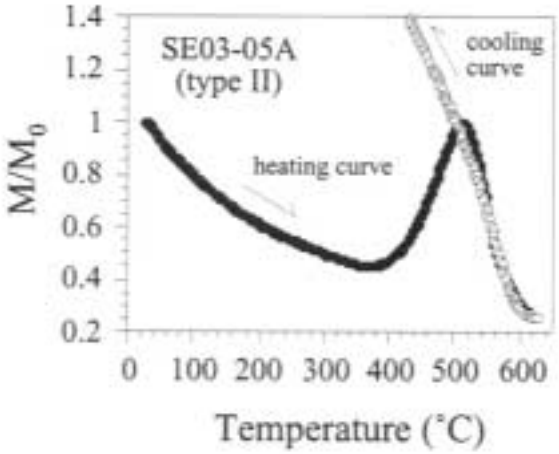

Fig. 6. Thermomagnetic curve of a type II sample, where magnetic iron sulphides where suspected to be present. See text for discussion.

weaker intensities and accounts for about 10% of the total *IRM*. The hard component is completely unblocked below 580°C and also has a distinctive drop of remanence at 340°C.

Low-temperature measurements of M_{rs} induced at 2.5 T and 10 K were conducted upon heating the sample back to room temperature after the removal of the applied field. Two heating runs were conducted, the first one involving previous cooling of the samples down to 10 K in the absence of any magnetic field (ZFC) and the second one involving the application of a 2.5 T field during initial cooling (FC) (Fig. 5). Low-T experiments indicate that both the ZFC and FC curves show evidence of a weak decay in magnetization at around 120 K. In addition, a sharp decrease of remanence is also observed below 40 K. A third, low-T experiment was performed by imparting M_{rs} in a 2.5 T field at room temperature. Variations of M_{rs} were later monitored upon cooling down to 20 K. All the studied samples undergo a marked decrease in M_{rs} below 40 K.

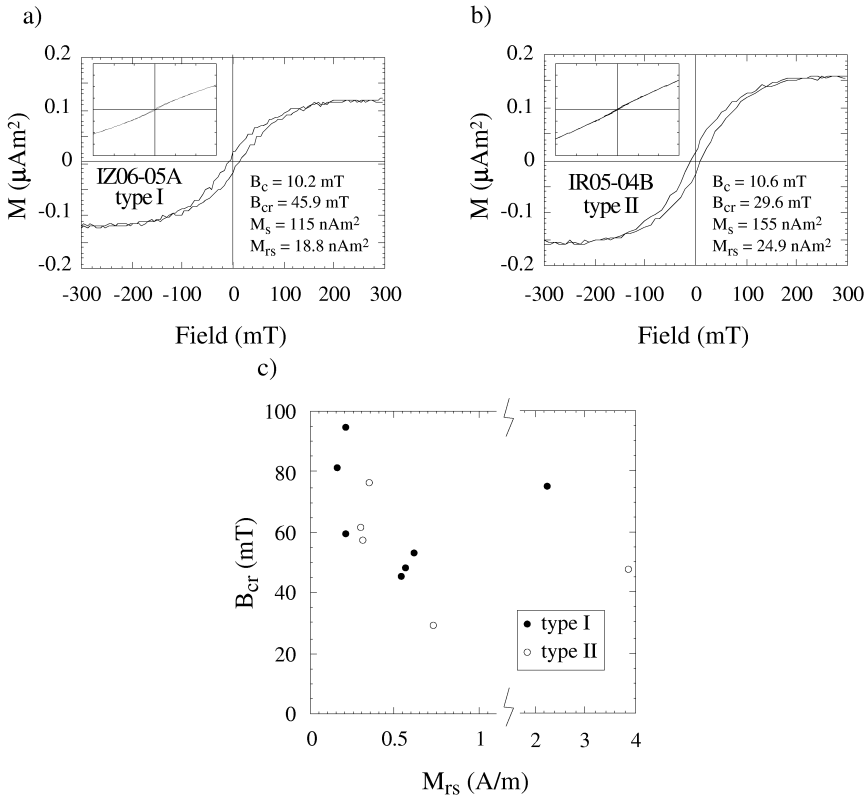

Fig. 7. a) Representative hysteresis loop for a type I sample. b) Representative hysteresis loop for a type II sample; hysteresis loops are shown before correction for the high-field paramagnetic slope (in the inset). d) Plot of M_{rs} versus B_{cr} for the studied samples. Solid (open) symbols indicate samples with type I (II) paleomagnetic behaviour.

Thermal alteration during thermomagnetic runs prevented identification of Curie points (Fig. 6), even when the experiments were carried out in a He atmosphere. Thermal breakdown is clear at ~ 400°C, which is also the temperature when a significant increase in low-field magnetic susceptibility is observed upon thermal treatment (Fig. 3). Cooling curves indicate that magnetite is produced as a result of the thermal breakdown. Below 400°C, the shape of the M_S heating curves is controlled by the contribution of paramagnetic minerals and no distinctive inflexion attributable to magnetic minerals is observed.

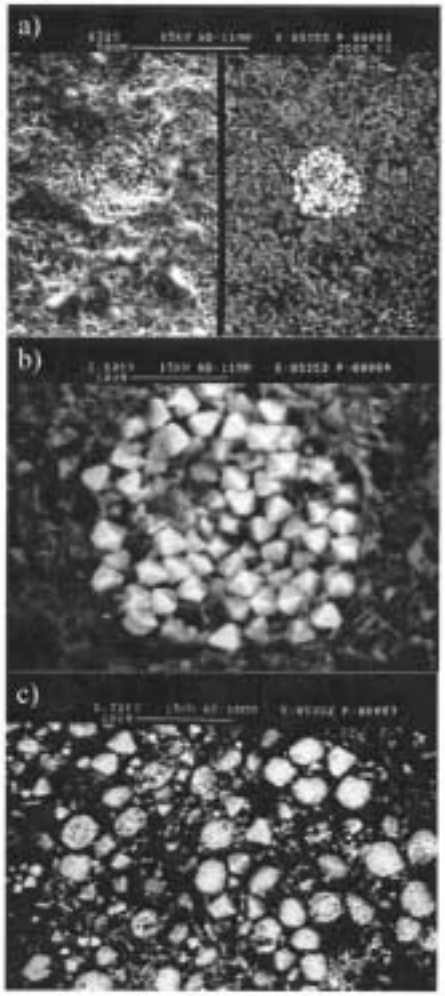

Fig. 8. SEM results from the PAF marls: a) Secondary electron and back-scattered electron image of an isolated pyrite framboid. b) Detailed view of the same framboid, showing well-defined octahedral crystals of up to 3 μm in length. c) Accumulation of framboids and euhedral crystals of pyrite. In the upper right-hand corner, both morphologies are filling the chambers of a foraminifer.

The high-field magnetization of the samples is mainly controlled by the paramagnetic fraction of the rocks (Fig. 7). Subtraction of the high-field paramagnetic contribution to the hysteresis curves reveals a weak ferromagnetic signal. B_{cr} values range between 29.6 and 95.1 mT. M_{rs} values are only occasionally higher than 1 A/m, and, below this value, there seems to be a negative correlation between B_{cr} and M_{rs} (Fig. 7c). Hysteresis parameters do not show a clear correlation with the type of paleomagnetic behaviour.

Any attempt to confirm the presence of magnetic minerals by means of conventional non-magnetic techniques have failed due to their low concentration in the PAF marls. Inspection of several thin sections indicates the ubiquitous presence of iron sulphide framboids dispersed in the rock matrix, which are commonly associated with organic matter and micro-fauna. SEM observations indicate that framboids are typically isolated and are spherical to sub-spherical in shape, ranging between 5 to 30 μm in diameter (Fig. 8). Framboids consist of aggregates of individual, well-defined octahedral crystals of 0.2–3 μm in length. Occasionally, euhedral crystals of up to 10 μm are also found. All the EDS analyses performed on framboids and euhedral crystals reveal that they consist of stoichiometric pyrite, as confirmed also by SAED patterns for a few selected samples. XRD analyses performed on rock-powder samples confirmed the presence of pyrite, but failed to identify any magnetic mineral.

5. DISCUSSION

5.1. Magnetic carriers

The unblocking temperatures of the *ChRM* suggest that magnetite is the main contributor to remanence in type I samples. *ChRM* directions after tectonic correction have normal and reversed polarity directions that are consistent with the Eocene reference direction for the studied area ($D = 5°$, $I = 52°$, $\alpha_{95} = 5.3°$; see *Taberner et al., 1999*) (Fig. 2a-c). The unblocking temperatures of the *ChRM* suggest that iron sulphides are the main remanence carriers in type II samples, with no significant contribution from magnetite. *ChRM* directions in type II samples also have normal and reversed directions consistent with the Eocene reference direction (Fig. 2d-e). The decay of remanence observed in several type I samples below 350°C suggests that small amounts of magnetic iron sulphides contribute to the *ChRM*. If so, the paleomagnetic directions that they record are broadly parallel to the directions identified above 350°C. These observations suggest that iron sulphides carry reliable *ChRM* directions in both type I and II samples. Because type II samples are less common than type I samples, and because they are often mixed at the outcrop scale, no significant field test can be performed for *ChRM* directions carried by iron sulphides only. Nevertheless, fold and reversal tests performed with the *ChRM* directions in localities where type I and II samples are present suggest that it represents an Eocene magnetization. An incremental fold test for the central sector of the studied area (Pamplona syncline) indicates that the best grouping of *ChRM* directions occurs at around 85–90% of unfolding (Fig. 9a). This grouping is, however, not significantly different than the 100% unfolding direction, which indicates that the *ChRM* was essentially acquired before tilting. A reversal test performed with *ChRM* directions in the same area is positive at the 95% confidence level and yields mean normal and reversed polarity directions consistent with an Eocene geocentric axial dipole direction (Fig. 9b).

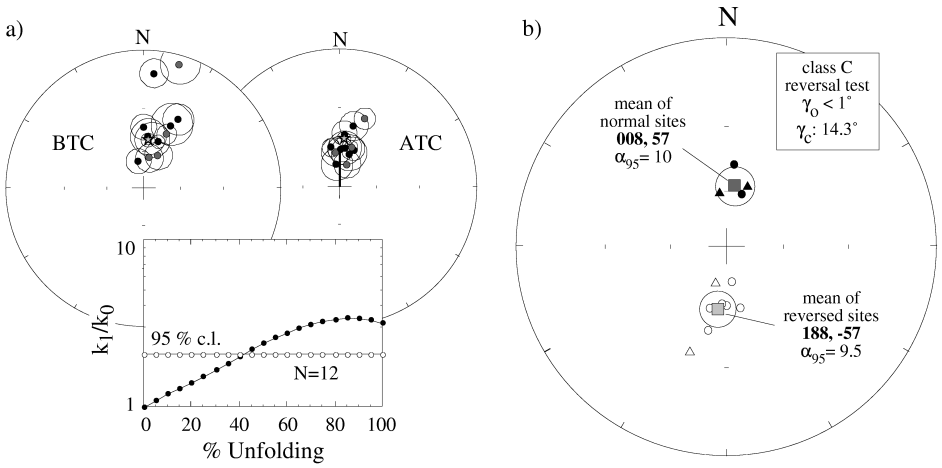

Fig. 9. a) Fold tests performed with site-mean *ChRM* directions in the Pamplona syncline. Black (grey) symbols indicate sites with predominance of type I (II+III) samples. Reversed polarity directions have been converted to their antipodal, normal polarity direction. The star indicates the Eocene reference direction. b) Reversal test performed for data from the Pamplona syncline. Circles (triangles) indicate sites with predominance of type I (II+III) samples.

Rock-magnetic experiments confirm the presence of magnetite and suggests the presence of magnetic iron sulphides in the studied marls. The presence of magnetite is demonstrated by the weakly expressed Verwey transition observed at ~ 120 K and by the unblocking temperatures of the *IRM* (< 580°C). Magnetite provides only a minor contribution to the hard (> 300 mT) component of the *IRM*, which indicates that it mainly contributes to the low coercivity fraction of the studied marls. The presence of small amounts of magnetic iron sulphides in the studied marls is indicated by the decay in the *IRM* observed below 340°C and by the relatively high coercivity values (up to 95 mT), which are similar to the values reported for greigite- and pyrrhotite-bearing sediment samples by *Roberts (1995)* and *Horng et al. (1998)* but higher than those reported for magnetite with a broad grain size distribution *(Dankers, 1978)*. The presence of high coercivity iron sulphides is also indicated by the relatively higher contribution of iron sulphides to the intermediate (40–300 mT) and hard (> 300 mT) *IRM* components. High coercivity magnetic iron sulphides might also account for the stronger resistance of *IRM* to AF demagnetization compared to *ARM*.

Identification of the iron sulphide responsible for the magnetic properties of the marls is not straightforward because pyrrhotite and greigite have similar magnetic properties. Perhaps the best way to discriminate between pyrrhotite and greigite in sediment samples is by their differential stability upon thermal treatment (*Krs et al., 1992*; *Roberts, 1995*; *Torii et al., 1996*; *Horng et al., 1998*) and by the presence of a low-*T* transition, which is observed for pyrrhotite, but not for greigite, below 35 K (*Dekkers et al., 1988; Rochette et al., 1990*; *Roberts, 1995*; *Torii et al., 1996*). Thermal decomposition of greigite becomes significant above 200°C (*Torii et al., 1996*) and is totally achieved below 350°C (*Krs et*

al., 1992; *Roberts, 1995*; *Torii et al., 1996*; *Horng et al., 1998*). In contrast, thermal instability in the PAF marls is only minor below 350°C and becomes significant above 400°C, which is in agreement with the breakdown of fine-grained (< 5 μm) pyrrhotite upon thermal treatment (*Dekkers, 1990*). However, thermal breakdown of pyrite is also significant above 400°C (*Passier et al., 2001*) and might also account for the high-temperature behaviour of the PAF marls. In any case, our results seem to rule out the presence of greigite as the magnetic iron sulphide in the marls. Concerning the low-*T* measurements, the sharp decrease of remanence below 40 K observed in the FC and ZFC curves might indicate the presence of pyrrhotite, although the loss of remanence might also have other causes (e.g., superparamagnetism, magnetic disordering of nanophase particles). The decay in M_{rs} observed below 40 K in the cooling curve suggests, however, that at least part of the drop of the M_{rs} at low temperatures might be due to pyrrhotite because SP magnetite and magnetic nanophases are not able to acquire a M_{rs} at room temperature.

5.2. Origin of magnetic minerals

Overall, rock magnetic data indicate the presence of magnetite and smaller amounts of magnetic iron sulphides, most likely pyrrhotite, in all the PAF samples studied. Due to the lack of direct observations of magnetic minerals, their origin has to be deduced on the basis of indirect information. Magnetite can have different sources such as bacterial synthesis, authigenic formation during diagenesis, or detrital provenance. The characteristic pattern of low-*T* M_{rs} behaviour below the Verwey transition, which is suggested to be indicative of aligned magnetite formed by magnetotactic bacteria (*Moskowitz et al., 1993*), was not observed. Also, bacterial magnetite is normally constrained to a narrow grain size spanning the SD state (e.g., *Oldfield, 1994*), which is not consistent with our hysteresis results. Thus, we rule out a biogenic origin for the detected magnetite. Burial diagenesis has been proposed to lead to authigenesis of magnetite at temperatures of 220°C (*Katz et al., 1998*). We also reject this origin for the magnetite since, in this case, the thickness of the studied rocks and overlying sediments cannot account for such high temperatures under a standard geothermal gradient. In the absence of a more plausible mechanism, we assume that the magnetite in the studied marls is detrital in origin.

In contrast, a detrital origin of magnetic iron sulphides is unlikely because iron sulphides are chemically and physically unstable during transport and sedimentation processes (*Berner, 1971*). Other explanations for the occurrence of magnetic iron sulphides, such as formation related to hydrocarbon seepage (*Reynolds et al., 1991*), formation of gas hydrates (*Housen and Musgrave, 1996*) or low-grade metamorphism (*Rochette et al., 1992*), can be also ruled out considering the geological setting of the PAF. The occurrence of pyrite framboids in the studied marls indicates that pyrite formed during early diagenesis, within the top few centimetres (< 1 m) of the sediment column located just below the redox surface separating oxic and anoxic conditions (*Sweeney and Kaplan 1973*; *Canfield and Berner, 1987*; *Berner 1984*). Our data suggest that magnetic iron sulphides carry a stable remanence that is consistent with the directions recorded by magnetite, a situation that has been reported in previous studies (e.g., *Roberts and Turner, 1993*; *Horng et al., 1998*). These observations suggest that magnetic iron sulphides

probably formed during early diagenesis as precursors of framboidal pyrite, and might therefore carry a *ChRM* that coexists with a detrital remanence carried by magnetite. According to the inferred maximum depth of 1 m at which iron sulphides form during early diagenesis, the delay between deposition of sediments and the lock-in of *ChRM* remanence in the PAF marls can be inferred to be of about 0.5–5 kyr considering mean accumulation rates between 5 and 50 cm/kyr. The PAF marls are therefore suitable for magnetostratigraphic and tectonic purposes, but not for detailed studies requiring time resolutions of less than ~ 10 kyr (e.g., polarity transitions, secular variation and geomagnetic excursions).

The observed paleomagnetic behaviour of the PAF marls is consistent with the proposed mechanism for *ChRM* acquisition. Minor contributions of iron sulphides to the *ChRM* in type I samples indicate that authigenic formation of iron sulphides, and the concomitant dissolution of magnetite that usually accompanies this process (e.g., *Canfield and Berner, 1987*; *Karlin 1990*; *Leslie et al., 1990*), was not widespread in samples belonging to this group. The *ChRM* in type II samples is mainly carried by magnetic iron sulphides, with negligible contribution from magnetite. This can be interpreted in terms of magnetite dissolution occurring as a result of an arrested pyritization process that enabled preservation of magnetic iron sulphides (*Roberts and Turner, 1993*). Furthermore, low *NRM* intensities above 300°C in type III samples suggests a small contribution of magnetite and/or iron sulphides to the remanence, which might have resulted from well-developed pyritization processes that caused pervasive dissolution of magnetite and prevented preservation of relict magnetic iron sulphides. Variations in sedimentation rates seem to control the paleomagnetic behaviour. Type I samples are more abundant in the lowermost levels, where low sedimentation rates (~ 5 cm/kyr; *Pueyo et al., 2002*) would favour oxic decomposition of organic carbon (*Canfield, 1994*) and thus prevent widespread formation and preservation of intermediate magnetic iron sulphides. Type II and III samples usually appear in the middle and upper stratigraphic levels, where sedimentation rates are well over 30 cm/kyr (*Pueyo et al., 2002*) and anaerobic processes would have been responsible for degradation of organic matter (*Canfield, 1994*). Under these conditions, the sediments would have supported active sulphate reduction and H_2S production, which would have resulted in formation of iron sulphides.

6. CONCLUSIONS

Paleomagnetic and rock-magnetic data indicate that magnetite and, to lesser extent, iron sulphides (most likely pyrrhotite), are the main carriers of the *ChRM* in Eocene marine marls of the Pamplona-Arguis Formation. Paleomagnetic data and SEM observations of pyrite textures suggest that the magnetic iron sulphides formed authigenically during a pyritization process that caused variable dissolution of (probably) detrital magnetite and preservation of magnetic iron sulphides. Both the magnetite and the magnetic iron sulphides appear to carry the same Eocene paleomagnetic direction as a result of a detrital remanence for magnetite and a *ChRM* for the iron sulphides. Stable remanences carried by early diagenetic magnetic iron sulphides are being increasingly reported in marine sediments and sedimentary rocks as old as Pliocene in age (e.g., *Linssen, 1988*; *Tric et al., 1991*; *Mary et al., 1993*; *Horng et al. 1998*). Our report adds to previous studies where magnetic iron sulphides of authigenic origin have been identified

in older rocks (e.g., *Krs et al., 1990*; *Roberts and Turner, 1993*; *Reynolds et al., 1994*), and therefore reinforces the view that magnetic iron sulphides are important contributors to the natural remanence of sediments and ancient sedimentary rocks (*Rochette et al., 1990*; *Verosub and Roberts, 1995*).

Acknowledgements: J.C.L. acknowledges financial support from the CSIC-DFG and the U.S. NSF (Visiting Fellowship), which enabled rock magnetic measurements at the Ludwig Maximilians University and the Institute for Rock Magnetism. We wish to thank the staff at both institutes, especially J. Marvin, N. Petersen and P. Solheid for their hospitality and help with the instruments and discussion of results. This work also benefited from discussion with H. Passier, E. Tohver, R. van der Voo and M. Dekkers. A. Roberts and an anonymous reviewer are also acknowledged for comments on an earlier version of the manuscript. Support for this work came from the Ph.D grants of the Gobierno de Navarra (J.C.L.) and the Ministerio de Educacion y Cultura (E.L.P.), and by the DGES (Projects PB96-0815 and PB98-1218).

References

Bentham P.A., 1992. *The Tectono-Stratigraphic Development of the Western Oblique Ramp of the South-Central Pyrenean Thrust System, Northern Spain*. Ph.D. Thesis, University of Southern California, Los Angeles.

Berner R.A., 1971. *Principles of Chemical Sedimentology*. Mc-Graw-Hill, New York.

Berner R.A., 1984. Sedimentary pyrite formation: an update. *Geochim. Cosmochim. Acta*, **48**, 605–615.

Burbank D.W., Vergés J., Muñoz J.A. and Bentham P., 1992a. Coeval hindward- and forward-imbricating thrusting in the south-central Pyrenees, Spain: timing and rates of shortening and deposition. *Geol. Soc. Am. Bull.*, **104**, 3–17.

Burbank D.W., Puigdefàbregas C. and Muñoz J.A., 1992b. The chronology of the Eocene tectonic and stratigraphic development of the eastern Pyrenean foreland basin, northeast Spain. *Geol. Soc. Am. Bull.*, **104**,1101–1120.

Canfield D.E., 1994. Factors influencing organic carbon preservation in marine sediments. *Chem. Geol.*, **114**, 315–329.

Canfield D.E. and Berner R.A., 1987. Dissolution and pyritization of magnetite in anoxic marine sediment. *Geochim. Cosmochim. Acta*, **51**, 645–659.

Canudo J.I., Molina E., Riveline J., Serra-Kiel J. and Sucunza M., 1988. Les événements biostratigraphyques de la zone prépyrénée d´Aragón (Espagne), de l´Eocene moyen á l´Oligocéne inférieur. *Rev. Micropal.*, **31**, 15–29 (in French).

Dankers P.H., 1978. *Magnetic Properties of Dispersed Natural Iron Oxides of Known Grain Size*. Ph.D. Thesis, University of Utrecht.

Dekkers M.J., 1990. Magnetic monitoring of pyrrhotite alteration during thermal demagnetization. *Geophys. Res. Lett.*, **17**, 779–782.

Dekkers M.J., Mattéi J.L., Fillion G. and Rochette P., 1988. Grain-size dependence of the magnetic behavior of pyrrhotite during its low-temperature transition at 34 K. *Geophys. Res. Lett.*, **16**, 855–858.

Dinarès-Turell J., McClelland E. and Santanach P., 1992. Contrasting rotations within thrust sheets and kinematics of thrust tectonics as derived from palaeomagnetic data: an example from the Southern Pyrenees. In: K.R. McClay (Ed.), *Thrust Tectonics*, Chapman and Hall, London, 265–276.

Dinarès-Turell J. and Dekkers M.J., 1999. Diagenesis and remanence acquisition in the Lower Pliocene Trubi marls at Punta di Maiata (southern Sicily): palaeomagnetic and rock magnetic observations. In: D.H. Tarling and P. Turner (Eds.), *Palaeomagnetism and Diagenesis in Sediments*, Geol. Soc. London, Special Publication, **151**, 53–69.

Florindo F. and Sagnotti L., 1995. Palaeomagnetism and rock-magnetism in the upper Pliocene Valle Ricca (Rome, Italy) section. *Geophys. J. Int.*, **123**, 340–354.

Hogan P.J., 1993. *Geochronologic, Tectonic and Stratigraphic Evolution of the Southwest Pyrenean Foreland Basin, Northern Spain*. Ph.D. Thesis, University of Southern California, Los Angeles.

Hogan P.J. and Burbank D.W., 1996. Evolution of the Jaca piggyback basin and emergence of the External Sierra, southern Pyrenees. In: P.F. Friend and C.J. Dabrio (Eds.), *Tertiary Basins of Spain*, Cambridge Univ. Press, Cambridge, 153–160.

Holl J.E. and Anastasio D.J., 1993. Paleomagnetically derived folding rates in the southern Pyrenees, Spain. *Geology*, **21**, 271–274.

Housen B.A. and Musgrave R.J., 1996. Rock-magnetic signature of gas hydrates in accretionary prism sediments. *Earth Planet. Sci. Lett.*, **139**, 509–519.

Horng C.-S. Torii M., Shea K.-S. and Kao S.-J., 1998. Inconsistent magnetic polarities between greigite- and pyrrhotite/magnetite-bearing marine sediments from the Tsailiao-chi section, southwestern Taiwan. *Earth Planet. Sci. Lett.*, **164**, 467–482.

Jiang W.-T., Horng C.-S., Roberts A.P. and Peacor D.R., 2001. Contradictory magnetic polarities in sediments and variable timing of neoformation of authigenic greigite. *Earth Planet. Sci. Lett.*, **193**, 1–12.

Karlin R., 1990. Magnetite diagenesis in marine sediments from the Oregon continental margin. *J. Geophys. Res.*, **95**, 4405–4419.

Katz B., Elmore R.D. and Engel M.H., 1998. Authigenesis of magnetite in organic-rich sediments next to a dike: implications for thermoviscous and chemical remagnetizations. *Earth Planet. Sci. Lett.*, **163**, 221–234.

Krs M., Krsová M., Pruner P., Zeman A., Novák F. and Jansa J., 1990. A petromagnetic study of Miocene rocks bearing micro-organic material and the magnetic mineral greigite (Sokolov and Cheb basins, Czechoslovakia). *Phys. Earth Planet. Inter.*, **63**, 98–112.

Krs M., Novák F., Pruner P., Kouklíková L. and Jansa J., 1992. Magnetic properties of greigite-smythite mineralization in brown-coal basins of the Krušné hory Piedmont, Bohemia. *Phys. Earth Planet. Inter.*, **70**, 273–287.

Larrasoaña J.C., Parés J.M., Millán H., DelValle, J. and Pueyo E.L., 2003. Paleomagnetic, structural and stratigraphic constraints on tranverse fault development during basin inversion: The Pamplona Fault (Pyrenees, N Spain). *Tectonics*, in press

Leslie B.W., Lund S.P. and Hammond D.E., 1990. Rock magnetic evidence of dissolution and authigenic growth of magnetic minerals within anoxic marine sediments of the California continental borderland. *J. Geophys. Res.*, **95**, 4437–4452.

Linssen J.H., 1988. Preliminary results of a study of four successive sedimentary reversal records from the Mediterranean. *Phys. Earth Planet. Inter.*, **52**, 207–231.

Lowrie W., 1990. Identification of ferromagnetic minerals in a rock by coercivity and unblocking temperature properties. *Geophys. Res. Lett.*, **17**, 159–162.

Mary C., Iaccarino S., Courtillot V., Besse J. and Aisaoui D.M., 1993. Magnetostratigraphy of Pliocene sediments from the Stirone river (Po Valley). *Geophys. J. Int.*, **112**, 359–380.

Millán H., Aurell M. and Meléndez A., 1994. Synchronous detachment folds and coeval sedimentation in the Prepyrenean External Sierras (Spain): a case study for a tectonic origin of sequences and system tracks. *Sedimentology*, **41**, 1001–1024.

Moskowitz B.M., Frankel R.B. and Bazylinski D.A., 1993. Rock-magnetic criteria for the detection of biogenic magnetite. *Earth Planet. Sci. Lett.*, **120**, 283–300.

Oldfield F., 1994. Toward the discrimination of fine-grained ferrimagnets by magnetic measurements in lake and near-shore marine sediments. *J. Geophys. Res.*, **99**, 9045–9050.

Passier H.F., de Lange G.J. and Dekkers M.J., 2001. Magnetic properties and geochemistry of the active oxidation front at the youngest sapropel in the eastern Mediterranean Sea. *Geophys. J. Int.*, **145**, 604–614.

Pueyo E.L., Millán H., Pocoví J. and Parés J.M., 1997. Cinemática rotacional del cabalgamiento basal surpirenaico en las Sierras Exteriores Aragonesas: datos magnetotectónicos. *Acta Geol. Hisp.*, **32**, 237–256 (in Spanish).

Pueyo E.L., Millán H. and Pocoví A., 2002. Rotation velocity of a thrust: a paleomagnetic study in the External Sierras (Southern Pyrenees). *Sedim. Geol.*, **146**, 191–208.

Pueyo E.L, Pocoví A., Parés J.M., Millán H. and Larrasoaña J.C., 2003. Thrust ramp geometries and spurious rotations of paleomagnetic vectors. *Stud. Geophys. Geod.*, **47**, 331–357.

Puigdefàbregas C., 1975. La sedimentación molásica de la cuenca de Jaca. *Pirineos*, **104**, 1–188 (in Spanish).

Reynolds R.L., Fishman N.S. and Hudson M.R., 1991. Sources of aeromagnetic anomalies over Cement Oil Field (Oklahoma), Simpson Oil Field (Alaska), and the Wyoming-Idaho-Utah Thrust Belt. *Geophysics*, **56**, 606–617.

Reynolds R.L., Tuttle M.N., Rice C.A., Fishman N.S., Karachewsky J.A. and Sherman D.M., 1994. Magnetization and geochemistry of greigite-bearing Cretaceous strata, North Slope Basin, Alaska. *Am. J. Sci.*, **294**, 485–528.

Roberts A.P., 1995. Magnetic properties of sedimentary greigite (Fe_3S_4). *Earth Planet. Sci. Lett.*, **134**, 227–236.

Roberts A.P. and Turner G.M., 1993. Diagenetic formation of ferrimagnetic iron sulphide minerals in rapidly deposited marine sediments, South Island, New Zealand. *Earth Planet. Sci. Lett.*, **115**, 257–273.

Rochette P., Fillion G., Mattéi J.L. and Dekkers M.J., 1990. Magnetic transition at 30–34 Kelvin in pyrrhotite: insight into a widespread occurrence of this mineral in rocks. *Earth Planet. Sci. Lett.*, **98**, 319–328.

Rochette P., Ménard G. and Dunn R., 1992. Thermochronometry and cooling rates deduced from single sample records of successive magnetic polarities during uplift of metamorphic rocks in the Alps (France). *Geophys. J. Int.*, **108**, 491–501.

Sweeney R.E. and Kaplan I.R., 1973. Pyrite framboid formation. Laboratory synthesis and marine sediments. *Econ. Geol.*, **68**, 618–634.

Taberner C., Dinarés-Turell J., Giménez J. and Docherty C., 1999. Basin infill architecture and evolution from magnetostratigraphic cross-basin correlations in the southeastern Pyrenean foreland basin. *Geol. Soc. Am. Bull.*, **111**, 2–21.

Teixell A., 1996. The Ansó transect of the southern Pyrenees: basement and cover thrust geometries. *J. Geol. Soc. London*, **153**, 301–310.

Torii M., Fukuma K., Horng C.-S. and Lee T.-Q., 1996. Magnetic discrimination of pyrrhotite- and greigite- bearing sediment samples. *Geophys. Res. Lett.*, **23**, 1813–1816.

Tric E., Laj C., Jéhanno C., Valet J.-P., Kissel C., Mazaud A. and Iaccarino S., 1991. High resolution record of the upper Olduvai transition from Po Valley (Italy) sediments: support for dipolar transition geometry? *Phys. Earth Planet. Inter.*, **65**, 319–336.

van Hoof A.A.M. and Langereis C.G., 1991. Reversal records in marine marls and delayed acquisition of remanent magnetization. *Nature*, **351**, 223–224.

Verosub K.L. and Roberts A.P., 1995. Environmental magnetism: past, present and future. *J. Geophys. Res.*, **100**, 2175–2192.

Weaver R., Roberts A.P. and Baker A.J., 2002. A late diagenetic (synfolding) magnetization carried by pyrrhotite: implications for paleomagnetic studies from magnetic iron sulphide-bearing sediments. *Earth Planet. Sci. Lett.*, **200**, 365–380.